

# 000 SUPPORTING HIGH-STAKES DECISION MAKING 001 002 THROUGH INTERACTIVE PREFERENCE ELICITATION 003 004 IN THE LATENT SPACE

005  
006 **Anonymous authors**  
007 Paper under double-blind review  
008  
009  
010  
011  
012

## ABSTRACT

013 High-stakes, infrequent consumer decisions, such as housing selection, challenge  
014 conventional recommender systems due to sparse interaction signals, heterogeneous  
015 multi-criteria objectives, and high-dimensional feature spaces. This work  
016 presents an interactive preference elicitation framework that utilizes preferential  
017 Bayesian optimization (PBO) to learn the unknown utility function of a user from  
018 pairwise comparisons that are observed and integrated in real-time. To increase  
019 efficiency in a complex feature space, we learn the preference model in the latent  
020 space of an autoencoder (AE). Additionally, to mitigate cold start, we obtain a  
021 personalized probabilistic prior through an automated user interview with a large  
022 language model (LLM). We evaluate the developed method on rental real estate  
023 datasets from two major European cities. The results show that executing PBO  
024 in the AE latent space improves final pairwise ranking accuracy by 12%. For  
025 LLM-based preference prior generation, we find that direct, LLM-driven weight  
026 specification is outperformed by a static prior, while probabilistic weight priors  
027 that use LLMs only to rank feature importance achieve 25% better pairwise accu-  
028 racy than a direct approach.

## 029 1 INTRODUCTION

030 User-tailored recommendations form a cornerstone of modern markets and online platforms, aiming  
031 to surface the most relevant options to reduce decision paralysis and increase click-through rates.  
032 Traditional recommendation approaches excel in entertainment or e-commerce domains, where user  
033 behavior generates abundant implicit feedback through clicks, purchases, and ratings. However,  
034 they struggle in sparse-feedback environments where users interact with only a handful of options  
035 before committing to one, motivating strategies for eliciting preferences in an interactive manner  
036 with as few interactions as possible. Such environments often correspond to high-stakes infrequent  
037 decisions characterized by complex heterogeneous multi-dimensional preference spaces, and have  
038 received little attention in the recommender system literature. We focus on the real estate market as  
039 an exemplary case study of an underexplored domain (Gharahighehi et al., 2021).  
040

### 041 1.1 RELATED WORK

042 **Classical Preference Elicitation** Traditional preference elicitation methods include conjoint analysis  
043 for estimating utilities over multi-attribute items (Arora & Huber, 2001) and multi-armed bandit  
044 approaches that balance exploration and exploitation (Parapar & Radlinski, 2021). Recent MAB  
045 extensions incorporate knowledge graphs to model inter-item relations and improve elicitation efficiency  
046 (Zhao et al., 2022). Preferential Bayesian optimization (PBO) adapts Bayesian optimization (BO)  
047 principles to scenarios lacking explicit objective functions, instead using implicit feedback  
048 like pairwise comparisons (González et al., 2017). Subsequent work has focused on developing  
049 acquisition functions that account for uncertainty in both model predictions and user responses (Astudillo  
050 & Frazier, 2020; Astudillo et al., 2023).  
051

052 **Preference Elicitation with LLMs** Large Language Model (LLM)-based preference elicitation  
053 follows two main approaches. Conversational methods enable dynamic natural language dialogue,

with methods like GATE allowing models to actively elicit user intent through open-ended interactions (Li et al., 2023; Andukuri et al., 2024). Structured approaches integrate LLMs within probabilistic frameworks, combining language models with Bayesian methods. One type of structured elicitation uses LLMs for user interaction and Bayesian methods for maintaining preference beliefs (Handa et al., 2024; Austin et al., 2024). Similar approaches fine-tune LLMs in a supervised manner with probabilistic models, yielding improved conversational preference elicitors (Piriyakulkij et al., 2023; Qiu et al., 2025). Here, Bayesian methods are only used for fine-tuning the model and do not directly aid in question selection and recommendation. Related work explores LLMs for decision support, constructing utility functions from stated user goals (Liu et al., 2024). It does not incorporate Bayesian methods but relies on Monte Carlo simulations for expected utility maximization. Existing work has focused on discrete feature spaces, such as category labels. For feature spaces with several continuous numerical dimensions, natural language representations are inefficient. To still leverage LLMs, we propose the use of open-ended conversations solely to generate personalized priors for downstream PBO tasks.

**Bayesian Optimization in High-Dimensional Spaces** Real-world recommendation scenarios frequently involve high-dimensional feature spaces that challenge conventional PBO approaches, as the search space grows exponentially with each additional dimension (Bellman, 1966). Two strategies address the curse of dimensionality in BO. The first explores lower-dimensional subspaces iteratively via one-dimensional subspace exploration for high-dimensional PBO (Tucker et al., 2020; Cheng et al., 2020). The second strategy performs optimization in learned low-dimensional latent spaces, such as combining preferential embeddings with BO to optimize only preference-relevant ( $\epsilon$ -effective) dimensions (Zhang et al., 2023). The embedding is facilitated through a randomly generated matrix before the main optimization loop. Another variant learns a low-dimensional feature space jointly with the response surface and a reconstruction mapping (Moriconi et al., 2020). The non-linear feature mapping is learned using Gaussian processs (GPs), thus achieving improved data efficiency. Lastly, variational autoencoders (AEs) have been used for molecular design with constraints to avoid invalid regions (Griffiths & Hernández-Lobato, 2020). The flexible degree of information compression via AEs is particularly valuable in high-dimensional feature spaces with a high degree of interdependence; however, to the best of our knowledge, the use of AEs has not been investigated in the context of interactive preference elicitation.

## 1.2 CONTRIBUTIONS

This work addresses the challenge of efficiently learning user preferences in high-dimensional, complex recommendation domains where direct preference specification is difficult, interaction data is sparse, and new data becomes available over time. We propose a comprehensive framework that couples PBO with user-specific LLM-based warm-start prior elicitation, and AE-based feature embeddings. This facilitates preference learning in a low-dimensional latent space while user interaction happens in a full-dimensional presentation space.

We evaluate our approach in the context of rental real estate recommendations. While this serves as an example for a challenging high-stakes domain, our approach generalizes to other domains with similar characteristics, such as the automotive or financial services markets. Based on LLM-based and statistics-based user simulations, we demonstrate that our framework outperforms vanilla PBO on two real-world datasets of the real estate markets in Madrid, Spain, and Munich, Germany, and the computation time meets real-time interactivity constraints.

The remainder of this paper is organized as follows. After introducing some preliminaries (Sec. 2), we pose our problem statement (Sec. 3.1) and detail the proposed framework (Sec. 3.2). This is followed by the evaluation of our case study (Sec. 4) and, finally, the conclusion (Sec. 5).

## 2 PRELIMINARIES

**Preference Learning** Preference learning is a subfield of machine learning concerned with inducing predictive models from empirical preference data. A preference can be conceptualized as a “*relaxed constraint which, if necessary, can be violated to some degree*” (Fürnkranz & Hüllermeier, 2011). Common approaches range from approximating individual utility functions to applying collaborative filtering across diverse user populations. Preference learning constitutes two pri-

108 many problem types: learning utility functions and learning preference relations (Fürnkranz &  
 109 Hüllermeier, 2011). A typical task involves learning a function that predicts preferences for an  
 110 unseen set of items, based on a known set of preferences. This work focuses on the object ranking  
 111 task. The objective is to learn a function that produces a total ordering of a set of objects without  
 112 access to explicit class labels – a form of unsupervised learning.  
 113

114 **Bayesian Optimization** BO provides a sample-efficient framework for global optimization of ex-  
 115 pensive, black-box functions. It places a probabilistic surrogate over the unknown objective and  
 116 uses an acquisition function to decide where to evaluate next, balancing exploration and exploitation  
 117 in a principled way (Frazier, 2018). We maximize an unknown function  $f : \mathcal{X} \rightarrow \mathbb{R}$  over a compact  
 118 feature space  $\mathcal{X} \subset \mathbb{R}^d$ . At iteration  $n$  we observe noisy evaluations  
 119

$$y_n = f(x_n) + \varepsilon_n, \quad \varepsilon_n \sim \mathcal{N}(0, \sigma^2),$$

120 and collect data  $\mathcal{D}_n = \{(x_i, y_i)\}_{i=1}^n$ . A common surrogate for the black-box function is a GP prior  
 121  $f \sim \text{GP}(m, k)$ , which yields a Gaussian posterior at any  $x$  with mean  $\mu_n(x)$  and variance  $\sigma_n^2(x)$   
 122 conditional on  $\mathcal{D}_n$ . The kernel  $k$  encodes smoothness and correlations. The subsequent evaluation  
 123 maximizes an acquisition function  $\alpha_n(x)$  that quantifies the value of sampling at  $x$ . These acquisi-  
 124 tions should be cheap to evaluate, and several options have been proposed in the literature (Brochu  
 125 et al., 2010; Astudillo et al., 2023; González et al., 2017). The loop alternates between updating the  
 126 surrogate with  $\mathcal{D}_n$ , maximizing  $\alpha_n(x)$  to choose  $x_{n+1}$ , evaluating  $y_{n+1}$ , and augmenting the data.  
 127 It terminates upon budget exhaustion or convergence, e.g., vanishing expected improvement. BO  
 128 excels in low to moderate dimensions and benefits from structural assumptions or dimensionality  
 129 reduction in high-dimensional spaces. Our framework builds on these foundations to incorporate  
 130 preference feedback.  
 131

132 **Preference Bayesian Optimization** Let  $f : \mathcal{X} \rightarrow \mathbb{R}$  be a black-box function, defined on a  
 133 bounded subset  $\mathcal{X} \subseteq \mathbb{R}^d$ . PBO aims to find (González et al., 2017, Eq. 1)  
 134

$$\mathbf{x}_{\min} = \arg \min_{\mathbf{x} \in \mathcal{X}} f(\mathbf{x}). \quad (1)$$

135 The assumption is that direct querying of  $f$  is infeasible, so we have to rely on pairwise comparisons  
 136 with two objects  $(\mathbf{x}_a, \mathbf{x}_b)$ , so-called duels. In each duel, we receive binary feedback, indicating  
 137 which object was selected. This dueling process is repeated until the uncertainty is reduced to a  
 138 satisfying amount. Utilizing BO techniques reduces the number of duels needed, and utilizing a  
 139 trained PBO model enables ranking of previously unseen items (González et al., 2017).  
 140

141 **Autoencoders** AEs are neural networks that learn compact latent representations by training an  
 142 encoder  $g_\theta : \mathbb{R}^d \rightarrow \mathbb{R}^r$  and a decoder  $h_\theta : \mathbb{R}^r \rightarrow \mathbb{R}^d$  to reconstruct inputs, where  $r \ll d$  is the  
 143 so-called latent dimension (Hinton & Salakhutdinov, 2006). Training minimizes a reconstruction  
 144 loss, such as mean squared error for continuous features or binary cross-entropy for binary features,  
 145 often with regularization (e.g., weight decay).  
 146

### 147 3 INTERACTIVE PREFERENCE ELICITATION FRAMEWORK

#### 148 3.1 PROBLEM STATEMENT

149 We define  $u : \mathcal{X} \rightarrow \mathbb{R}$  as the unknown utility function of a user, defined on the feature space  $\mathcal{X} \subset \mathbb{R}^d$ .  
 150 A corresponding pairwise preference function  $F_u : \mathcal{X} \times \mathcal{X} \rightarrow \{0, 1\}$  maps any pair of data points  
 151  $(x, x')$  to a binary response, indicating which option is preferable. Our goal is to obtain a proba-  
 152 bilistic model  $\hat{u}^*$  from a parametric class  $\mathcal{U}_\theta$  with a corresponding pairwise preference probability  
 153 distribution  $F_{\hat{u}}$ , such that  
 154

$$\hat{u}^* = \arg \min_{\hat{u} \in \mathcal{U}_\theta} \mathbb{E}_{(x, x') \sim \mathcal{X}^2} \left[ L(F_u(x, x'), F_{\hat{u}}(x, x')) \right], \quad (2)$$

155 where  $L$  is an appropriate loss function. Note that our problem is intentionally framed as an object  
 156 ranking task, rather than finding an optimal feature vector. The reason is that only a finite number  
 157 of items, i.e., samples from the feature space, representing real assets, are selectable. Further, while  
 158 a set of items  $\mathcal{I} = \{x_1, \dots, x_{|\mathcal{I}|}\}$  is known at the time of preference elicitation, new options might  
 159 be unveiled over time. The learned preference model should also be able to rank these accurately.  
 160

162 We assume a channel through which we can query the user by proposing pairwise comparisons and  
 163 obtaining binary feedback. In a realistic setting, the number of queries is limited by an unknown  
 164 budget  $N \in \mathbb{N}$ . Therefore, we aim to model the utility function of the user as accurately as possible  
 165 with the fewest queries possible.

166

### 167 3.2 PREFERENCE BAYESIAN OPTIMIZATION IN THE LATENT SPACE

168

169 Our approach leverages AEs to decouple the optimization space from the presentation space in PBO,  
 170 by performing BO in the latent space of the AE, which provides a more efficient representation of  
 171 the original feature space. A well-trained encoder ideally removes correlated features, captures non-  
 172 linear relationships, and distills the input into its most relevant components. Optimization in this  
 173 reduced space should converge more rapidly while maintaining representational resolution. In sum-  
 174 mary, we learn a utility surrogate  $\hat{u}: \mathcal{Z} \rightarrow \mathbb{R}$  with the corresponding pairwise preference function

$$175 F_{\hat{u}}(x, x') = \begin{cases} 1 & \text{if } \hat{u}(g_{\theta}(x)) \geq \hat{u}(g_{\theta}(x')), \\ 0 & \text{otherwise,} \end{cases} \quad (3)$$

176

177 where  $g_{\theta}$  is the encoder of the AE trained on the set of available items  $\mathcal{I}$ . The associated encoder  
 178 is denoted as  $h_{\theta}$ . The autoencoder is trained with normalized features, which is why we apply  
 179 normalization before passing a data point to the encoder and denormalization before displaying a  
 180 decoded item to the user. For clarity, we do not include these steps in our formalization. In addition  
 181 to the following textual description, our approach is formalized in Algorithm 1.

182

#### 183 3.2.1 UTILITY PRIOR ESTIMATION USING LLMs

184

185 In PBO, selecting informative duels is particularly important during the early stages of elicitation  
 186 (Handa et al., 2024; Brochu et al., 2010), and an unsuitable starting point could waste valuable query  
 187 budget. To mitigate this cold-start issue, we aim to find a maximally informative prior to initialize  
 188 the preference model. This is achieved by evaluating  $M$  pairwise preference decisions based on a  
 189 synthetic utility function surrogate. We use a standard linear model  $u_{\text{syn}}(x) = w^T x$ , where the prior  
 190 weights  $w$  are obtained through an LLM-guided user interview instead of relying on a predefined  
 static weight vector.

191 **User Interview** The LLM is assigned the persona of a domain-specific interviewer. Apart from  
 192 reaching the query budget, the conversation can also conclude when the LLM determines it has  
 193 gathered sufficient information or when the user explicitly indicates they are finished. The obtained  
 194 preference information  $\pi$  either directly contains the utility model weights  $w = \pi$  or a ranking for the  
 195 probabilistic initialization explained below. Additionally, lower and upper bounds  $\underline{x}, \bar{x}$  of the feature  
 196 subspace that is acceptable for the user are returned by the LLM. Including hard constraints can  
 197 make the elicitation process significantly more efficient by ensuring that all presented comparisons  
 198 fall within the feasible decision space of the user. An example output of the LLM for the real estate  
 199 domain could look like the following:

- 200 1. **Lower bounds** on essential criteria, including the minimum floor level, required living area  
 201 in square meters, and available parking spaces.
- 202 2. **Upper bounds** for constraining criteria such as maximum acceptable total monthly rent  
 203 and maximum acceptable travel time to the workplace.
- 204 3. **Feature importance weights** representing the relative significance of each feature in the  
 205 decision-making process. The LLM estimates these weights based on the conversation.

207 **Probabilistic Weight Initialization** Instead of directly returning utility function weights, we em-  
 208 ploy an approach based on the work in (Handa et al., 2024) which asks the LLM to rank features in  
 209 order of importance – a task that aligns better with demonstrated strengths of LLMs in comparative  
 210 reasoning and ordinal relationships. This approach works by sampling feature weights from nor-  
 211 mal distributions whose parameters are informed by both the ranking of the LLM and the inherent  
 212 variance structure of the data. For each feature  $i$  with rank  $r_i$  (where lower ranks indicate higher  
 213 importance), the weight  $w_i$  is sampled from:

$$214 \quad 215 w_i \sim \mathcal{N} \left( 0, \alpha \cdot \frac{\sigma_i^2}{\max_{j \in \{0, \dots, d\}} (\sigma_j^2)} \cdot \frac{1}{r_i} \right), \quad (4)$$

216 where  $\sigma_i^2$  represents the variance of feature  $i$  before normalization, and  $\alpha$  is a scaling factor that  
 217 controls the overall magnitude of the weights. The intuition behind this approach is that features  
 218 deemed more important by the user (receiving lower rank values) should have larger potential weight  
 219 magnitudes, while features with higher natural variance already exhibit significant influence on the  
 220 decision space and thus warrant proportionally scaled weights. Different from Handa et al. (2024),  
 221 we add  $\frac{1}{\max_{j \in \{0, \dots, d\}}(\sigma_j^2)}$  as a normalization term ensuring that features with exceptionally large  
 222 variances do not receive disproportionately large weights regardless of their actual importance to the  
 223 user. The corresponding prompt for our case study is provided in the Appendix (Sec. A.3.3).  
 224

225 **Warm-Start Dataset** After the weights for the synthetic model  $u_{\text{syn}}(x)$  have been determined, we  
 226 sample  $M$  item pairs from  $\mathcal{I}$  uniformly at random. For each pair  $(x, x')_k$ , we evaluate the associated  
 227 pairwise preference function to obtain the binary feedback

$$y_k = F_{u_{\text{syn}}}(x_k, x'_k) = \begin{cases} 1 & \text{if } u_{\text{syn}}(x) \geq u_{\text{syn}}(x'), \\ 0 & \text{otherwise.} \end{cases} \quad (5)$$

231 Since the probabilistic preference model is trained in the latent space, we compute the dataset of  
 232 embedded observations

$$\mathcal{D} = \left\{ (g_{\theta}(x_k), g_{\theta}(x'_k), y_k) \right\}_{k=0}^M \quad (6)$$

235 as well as the embedded lower and upper bounds of the feasible feature subspace  $\underline{z} = g_{\theta}(\underline{x}), \bar{z} =$   
 236  $g_{\theta}(\bar{x})$ .

### 3.2.2 ELICITATION LOOP

239 Denoting the  $n^{\text{th}}$  update of the probabilistic utility model  $\hat{u}$  based on new observation data  $\mathcal{B}$  as  
 240  $\hat{u}_n = \text{Fit}(\hat{u}_{n-1}, \mathcal{B})$ , we initialize  $\hat{u}$  using the warm-start dataset as  $\hat{u}_M = \text{Fit}(\hat{u}_0, \mathcal{D})$ , where  
 241  $\hat{u}_0 \sim \text{GP}(\cdot, \cdot)$  represents an arbitrary naive prior distribution. From hereon, the approach fol-  
 242 lows the principle of PBO. Until the query budget  $N$  is reached, we determine each new query  
 243  $(z_k, z'_k)$  by maximizing an acquisition function  $\alpha_k(z_k, z'_k)$ . The user is shown the decoded query  
 244  $(h_{\theta}(z_k), h_{\theta}(z'_k))$  in the presentation space and their preference choice  $y_k$  is recorded. The prefer-  
 245 ence model is then updated as  $\hat{u}_k = \text{Fit}(\hat{u}_{k-1}, \{(z_k, z'_k, y_k)\})$ . In the following two paragraphs,  
 246 we describe the utility model update and the acquisition function optimization in more detail.  
 247

248 **Utility Model Update** The probabilistic utility surrogate  $\hat{u}(z)$  is modeled by a specialized GP  
 249 model based on the work in (Chu & Ghahramani, 2005). Since users interact in the presentation  
 250 space, they express preferences over reconstructions of latent items  $\hat{x} = h_{\theta}(z)$ . When a user ex-  
 251 presses a preference for an item  $\hat{x}$  over  $\hat{x}'$ , the model interprets this as evidence that  $u(x) > u(x')$ .  
 252 The likelihood of this preference is modeled using a probit function:

$$Pr(x \succ x') = \Phi\left(\frac{\hat{u}(z) - \hat{u}(z')}{\sigma}\right), \quad (7)$$

255 where  $\sigma$  captures user preference inconsistency as well as noise from the AE reconstruction error,  
 256 and  $\Phi$  is the cumulative distribution function of a standard normal distribution. The theoretical basis  
 257 for this noise model is discussed in the Appendix (Sec. A.1). The resulting posterior distribution  
 258 is not analytically tractable since the probit likelihood is non-conjugate with the Gaussian process  
 259 prior. Therefore, the model employs a Laplace approximation that finds the maximum a posteriori  
 260 estimate of the latent utility values and then forms a Gaussian approximation to the posterior  
 261 centered at this mode (Chu & Ghahramani, 2005).

262 **Acquisition Function Optimization** In BO, each sample, i.e., user query, is determined by an  
 263 acquisition function, optimizing the value gained through the corresponding observation. For our  
 264 approach, we choose the expected utility of the best option (qEUBO) acquisition function, which is  
 265 defined as (Astudillo et al., 2023, Sec. 4.1)

$$\text{qEUBO}_n(z, z') = \mathbb{E}_n \left[ \max \{ \hat{u}(z), \hat{u}(z') \} \right], \quad (8)$$

269 where  $\mathbb{E}_n$  denotes the conditional expectation given our observations of user preference choices after  
 $n$  queries. Since  $\hat{u}$  is modeled as a Gaussian distribution, qEUBO <sub>$n$</sub>  can be efficiently maximized

270 via a single-sample approximation (Lin et al., 2022, Sec. 4.3). While this, in principle, supports the  
 271 integration of arbitrary feature space constraints (Balandat et al., 2020), we focus on feature-wise  
 272 lower and upper bounds  $z \in [\underline{z}, \bar{z}]$  that can efficiently be extracted during our LLM-based prior  
 273 estimation (see Sec. 3.2.1).

274

### 275 3.3 EXTENSION FOR CONTINUAL AE IMPROVEMENT

276

277 In a scenario in which new items might become available over time, one might want to leverage  
 278 the opportunity to retrain and improve the used AE with an expanded input dataset. We outline a  
 279 corresponding continual approach in the following: Consider the trained AE with encoder  $g_\theta$  and  
 280 decoder  $h_\theta$ , initially trained on a set of items  $\mathcal{I}$ . During elicitation, the AE is used in generating a  
 281 user-feedback dataset  $\mathcal{D}_\theta = \{(z_0, z'_0, y_0), \dots\}$  for the construction of the utility function surrogate  
 282  $\hat{u}_\theta$ . When training a new AE, we obtain an updated encoder  $g_{\theta^\circ}$  and decoder  $h_{\theta^\circ}$  on an expanded  
 283 dataset  $\mathcal{I}^\circ \supset \mathcal{I}$ . To avoid losing previously collected feedback, we re-embed the user-feedback  
 284 dataset by mapping the old latent representations through the old decoder and the new encoder:  
 285  $\mathcal{D}_{\theta^\circ} = \{(g_{\theta^\circ}(h_\theta(z_0)), g_{\theta^\circ}(h_\theta(z'_0)), y_0), \dots\}$ . This re-embedded dataset enables us to rerun the  
 286 PBO flow, yielding an updated utility function surrogate  $\hat{u}_{\theta^\circ}$ .

287

## 288 4 EVALUATION

289

### 290 4.1 DATASETS

291

292 We evaluate our method using the *Idealista18* open-source real-estate dataset (Rey-Blanco et al.,  
 293 2024). It comprises geo-referenced data of residential real-estate listings from the year 2018  
 294 for Spain’s three largest cities – Madrid (94,815 listings), Barcelona (61,486), and Valencia  
 295 (33,622). Each listing is accompanied by property attributes (e.g., price, unit price, number of  
 296 rooms/baths, constructed area, presence of a terrace, lift, pool, garden, etc.), spatial coordinates (lat-  
 297 itude/longitude, with modest anonymization), and supplemental data drawn from cadastral records  
 298 (building quality, construction year, dwelling counts, etc.). The dataset also includes neighborhood  
 299 polygons for each city with official boundaries and a set of point of interests (POIs) per city: coordi-  
 300 nates of the city center, main streets, and metro stations. For the sake of this evaluation, we utilize all  
 301 Madrid listings with a manual selection of 12 features, focusing on property attributes. A detailed  
 302 overview is given in Appendix A.4, (Table 4). All analyses and results presented in Section 4.3,  
 303 are based on this publicly available dataset. In addition, we created a comparable dataset for the  
 304 city of Munich, Germany. It contains about 1,500 rental real-estate listings with their corresponding  
 305 metadata, alongside free-text information from the descriptions. Additionally, we utilize geospatial  
 306 analysis to compute additional information, such as proximity to the nearest public transport stop  
 307 or the average surrounding noise level. While we are unable to publish the dataset at this point due  
 308 to licensing restrictions, we report our evaluation results in Appendix A.4, Table 6. Notably, these  
 309 results are in line with the findings reported in Section 4.3.

310

### 311 4.2 SETUP

312

**313 AE Training** We employ robust scaling techniques that use interquartile ranges rather than mean  
 314 and standard deviation, making the normalization less sensitive to outliers. Additionally, median  
 315 value imputation handles missing or malformed values, and outliers are removed by clipping the  
 316 data at the 1st and 99th percentiles. The tuned architecture has two hidden layers in both the encoder  
 317 and decoder and six latent features. We use hyperbolic tangent (*tanh*) as the activation function. The  
 318 full set of hyperparameters is provided in Appendix A.5, Table 8.

319

**320 User Simulation** Generating responses that approximate human preferences well is a challenging  
 321 task. Specifically for content recommendation, it was found that biographical sketches of hypotheti-  
 322 cal people are well-suited for simulating human decision makers (Li et al., 2023) with LLMs. Based  
 323 on these findings, we prompt a state-of-the-art LLM with thinking capabilities to choose which of  
 324 two properties, represented by a textual representation of their feature vectors, it prefers, given the  
 325 description of a persona. In order to cover the complete elicitation process, the LLM is also used  
 326 to acquire probable strict constraints (lower or upper bounds of features) as well as a feature weight

prior. Our primary evaluation uses the closed-source model Gemini-2.5-Flash-Lite<sup>1</sup> and we conduct an ablation experiment using the open-source model gpt-oss-120b OpenAI et al. (2025). The utilized prompt is provided in Appendix A.3.3.

In addition to simulating human responses using LLMs, we implement a more analytical approach based on a linear utility function model  $\hat{u}_\theta$ . Here, a weight vector  $\theta \in [-1, 1]^d$ ,  $\|\theta_i\|_1 = 1$  is used to approximate the preferences of a user. We use a range of preset profiles, which are then randomized using uniformly sampled offsets, between -0.5 and 0.5, added to each specified weight. We use the obtained model to make pairwise comparison decisions based on the Bradley-Terry model of human preferences (van Berkum, 1997; Hunter, 2004). Accordingly, the likelihood of a property  $x$  being preferred over a property  $x'$  is defined by

$$Pr(x \succ x' | u_\theta) = \frac{1}{1 + e^{(u_\theta(x') - u_\theta(x))}}.$$

The statistical profiles and LLM personas have been chosen such that they roughly represent the same preferences and tendencies. For example, the *budget-conscious* profile and the *student* persona encode the same preference for an ideally low rent and proximity to the city center. Personas and profiles are derived from survey studies Walker & Li (2007); Lee et al. (2019) and confirmed by domain experts to be relevant classes of stakeholders in the rental real estate market. The detailed weights and persona prompts are provided in the Appendix (A.3.4). The static prior is hand-crafted to represent a reasonable preference profile and provided in Table 3.

**Evaluation Parameters** For both variations of the benchmark – LLM-based and statistics-based – we use a randomly generated test set to serve as ground truth for evaluating the model performance after every training step. This test set consists of  $n = 50$  randomly sampled items from our data set, serving as the items to be ranked. The test set is reused for all runs of the same persona or profile across one evaluation. The learned preference model is never given access to the test set, since we only use the posterior of the model for evaluation. Every result is reported based on 200 evaluation runs, split into using either the LLM-based or statistics-based user simulation. Every persona or profile is chosen equally, equating to 25 runs per persona or profile, as we define four personas and four profiles for our scenario. For one evaluation run, we select an initialization budget of  $M = 5$  and a query budget of  $N = 25$ . Additionally, we test a totally random prediction strategy to establish a baseline.

We use two primary metrics to measure the performance of the elicitation methods. First, we calculate the pairwise accuracy, which is the fraction of correctly ordered pairs between the predicted and ground-truth preferences. Secondly, we employ normalized discounted cumulative gain (NDCG), a utility-dependent measure of ranking quality that gives more weight to items ranked higher in the list Järvelin & Kekäläinen (2002). It is defined based on the discounted cumulative gain (DCG) at position  $k$ :

$$DCG@k = \sum_{i=1}^k \frac{rel_i}{\log_2(i+1)}, \quad (9)$$

where  $rel_i$  is the relevance score of the item at position  $i$  in the predicted ranking. DCG@k is normalized by the ideal discounted cumulative gain (IDCG@k), which is the DCG score of a perfectly sorted list, to obtain

$$NDCG@k = \frac{DCG@k}{IDCG@k}. \quad (10)$$

Essentially, NDCG@k measures how much of the maximum possible utility was captured in the top  $k$  positions, relative to an ideal ranking for that query. We generally report the mean and 95% parametric confidence intervals across all runs.

### 4.3 RESULTS

Figure 1 visualizes the performance differences between our proposed approach (combining PBO with AEs and LLMs), the random ranking baseline, and vanilla PBO. Our method requires LLM-

<sup>1</sup><https://storage.googleapis.com/deepmind-media/Model-Cards/Gemini-2-5-Flash-Lite-Model-Card.pdf>

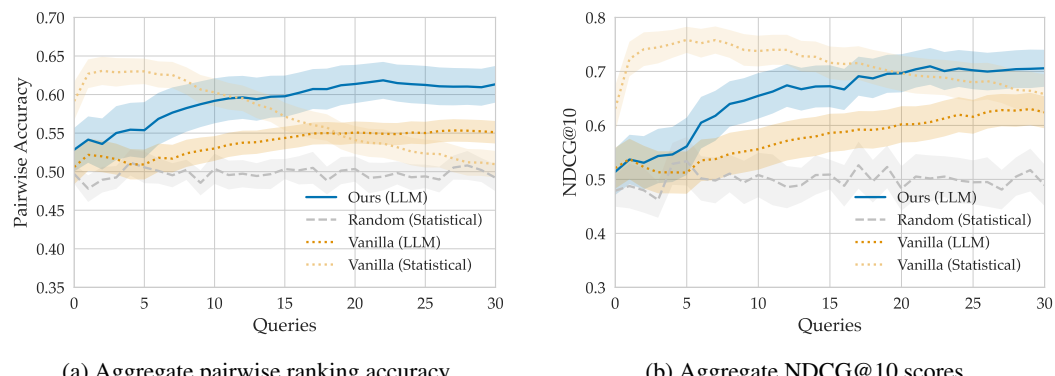


Figure 1: Aggregated scores over time for random ranking, vanilla PBO (both user simulation types), and our proposed approach. Shaded areas represent 95% confidence intervals over 200 runs each.

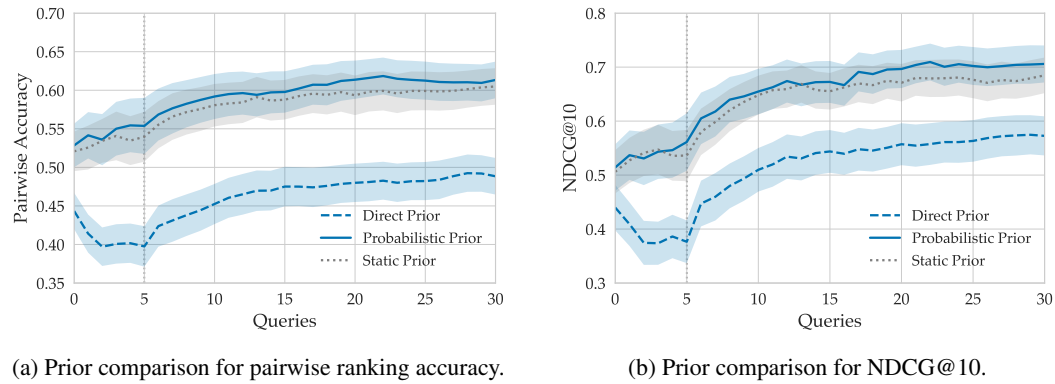


Figure 2: Comparison of PBO+AE performance using three different prior initialization methods. The probabilistic LLM-based prior slightly outperforms the static prior, while the direct LLM-based prior yields the worst results.

based simulation for evaluation, as it elicits probabilistic priors from simulated users. Vanilla PBO accommodates both simulation approaches. PBO runs with statistical simulation achieve higher initial scores but experience rapid decline after a few iterations. This strong initial performance is likely the result of overlap between profile weights and the default static prior used in evaluation. Under LLM-based simulation with noisier signals, our approach consistently outperforms vanilla PBO. Our method achieves average final pairwise accuracy of  $0.613 \pm 0.024$  and average NDCG@10 score of  $0.706 \pm 0.034$ . These results represent 13.7% and 13.5% improvements over vanilla PBO under LLM-based simulation, respectively. A noteworthy observation in Figure 1 is that vanilla PBO in the statistical simulation shows the counterintuitive behavior of an initial rapid increase in accuracy followed by a monotone decrease until the end of the elicitation loop. This indicates overfitting to a certain region of the feature space, which is likely a consequence of the high dimensionality and associated issues of overconfident estimates and premature exploitation.

The performance improvement incurs an average overhead of 358ms per optimization step compared to vanilla PBO. Additionally, we measure candidate diversity to ensure the decoder output does not collapse to similar objects. We define candidate diversity as the mean feature-wise standard deviations across candidates generated during acquisition function optimization, measured in presentation space. We observe no significant difference between PBO and PBO+AE methods. Table 1 presents detailed aggregated evaluation results.

A similar performance pattern emerges when applying our method to the Munich rental real estate dataset (Appendix A.4: Tables 5, 6). Although the pairwise ranking accuracy is slightly lower on this smaller dataset, the NDCG@10 scores are comparable. Crucially, PBO+AE again demonstrates better predictive performance over vanilla PBO. This suggests that our approach effectively learns

432 Table 1: Comparison of evaluation metrics across all approaches and user simulation variants.  
433

434 Method	435 Simulation	436 Prior	437	438 Pairwise Acc.	439 NDCG@10	440 Cand. Diversity	441 Runtime/iter (ms)
436 PBO	437 LLM	438 Static	439	440 $0.539 \pm 0.014$	441 $0.622 \pm 0.026$	442 $0.775 \pm 0.116$	443 $518 \pm 10$
		444 Statistical	445 Random	446 $0.492 \pm 0.017$	447 $0.489 \pm 0.038$	448 $1.078 \pm 0.040$	449 $0 \pm 0$
		450 Static	451	452 $0.510 \pm 0.017$	453 $0.658 \pm 0.037$	454 $0.633 \pm 0.060$	455 $304 \pm 12$
456 PBO + AE	457 LLM	458 Direct Elicit	459	460 $0.488 \pm 0.024$	461 $0.573 \pm 0.036$	462 $0.664 \pm 0.057$	463 $641 \pm 65$
		464 Prob Elicit	465	466 $0.613 \pm 0.024$	467 $0.706 \pm 0.034$	468 $0.596 \pm 0.066$	469 $876 \pm 216$
		470 Static	471	472 $0.605 \pm 0.024$	473 $0.685 \pm 0.033$	474 $0.611 \pm 0.064$	475 $723 \pm 99$
	476 Statistical	477 Static	478	479 $0.556 \pm 0.025$	480 $0.584 \pm 0.037$	481 $0.613 \pm 0.039$	482 $465 \pm 84$

444 preferences even for high-dimensional datasets of a smaller size. Additionally, we provide the aggregated results from utilizing the open-source LLM in Appendix A.4, Table 7. While we observe 445 generally worse performance of all variants compared to the closed-source LLM, our approach still 446 outperforms vanilla PBO. Further, the usefulness of warm starting is demonstrated in Appendix A.4, 447 Figure 4, which shows that PBO+AE with cold start quickly plateaus and performs worse than our 448 proposed approach at the end of the elicitation process. 449

450 **LLM Prior Impact** Figure 2 ablates all three initialization strategies for PBO+AE: a fixed static 451 prior, a directly elicited LLM prior (point estimate), and a probabilistically elicited LLM prior that 452 samples weights from a distribution informed by an LLM-produced feature ranking (Sec. 3.2.1). The 453 first five queries use synthetic comparisons generated under the respective prior (vertical marker), 454 after which the model observes simulated user feedback. Feature-wise bounds are active and identical 455 across the LLM-based variants. The static prior runs use wider dataset-level bounds instead. Across 456 200 runs for all personas, the probabilistic prior yields the best sample efficiency and the highest 457 final performance on pairwise accuracy and NDCG@10. The direct prior shows an early drop – 458 consistent with overconfident misspecification – and never closes the gap. At the query budget limit, 459 PBO+AE with probabilistic elicitation achieves  $0.613 \pm 0.024$  pairwise accuracy and  $0.706 \pm 0.034$  460 NDCG@10, slightly but consistently outperforming the static prior and clearly surpassing the direct 461 prior. These results indicate that an uncertainty-aware prior based on LLM guidance is more robust 462 and provides a sustained advantage once real user feedback arrives. We hypothesize that the static 463 prior shows comparatively strong results because it is likely a good fit for most personas. For 464 example, the relatively strong preference for a lower price encoded in the static weight prior is likely to 465 match the preferences of every persona. This effect is unlikely to generalize to a larger population 466 of users. 467

#### 468 4.4 LIMITATIONS

469 Our evaluation has several limitations. The LLM-based personas used in our simulations may not 470 accurately reflect authentic human decision-making, and they represent only a limited number of 471 stereotypical users. LLM responses are not fully consistent across queries, even with low temperature 472 settings. Our datasets are from two major European cities, which limits their generalizability to 473 other geographic markets or cultural contexts. The selected features (e.g., bikeability scores, public 474 transport access) reflect local urban characteristics that may not be applicable to different settings 475 or recommendation domains, such as automotive purchases. Additionally, our reliance on pairwise 476 accuracy as the primary evaluation metric may not fully capture user satisfaction, as real users often 477 value factors beyond ranking accuracy, such as diversity, novelty, or serendipity. 478

## 479 5 CONCLUSION

480 This work demonstrates that combining preferential Bayesian optimization with LLM-guided priors 481 and autoencoder-based dimensionality reduction effectively addresses preference learning challenges 482 in high-stakes, sparse-interaction domains. Our approach achieves substantial accuracy 483 improvements compared to vanilla preferential Bayesian optimization on rental market datasets from 484 two European cities. This framework has immediate applications for online real estate platforms, 485 where it could reduce user fatigue by minimizing the number of property comparisons needed to

486 identify suitable options. Beyond rental real estate, further real-world applications are high-stakes  
487 decisions, e.g., job searches or major purchases, where sparse interaction data limits traditional  
488 recommender systems. Key directions for future work include multi-stakeholder preference aggre-  
489 gation (e.g., couples searching together), temporal adaptation for evolving preferences, investigation  
490 of other decision domains, and empirical validation with human users.

491

492

493

494

495

496

497

498

499

500

501

502

503

504

505

506

507

508

509

510

511

512

513

514

515

516

517

518

519

520

521

522

523

524

525

526

527

528

529

530

531

532

533

534

535

536

537

538

539

## 540 REFERENCES

542 Chinmaya Andukuri, Jan-Philipp Fränken, Tobias Gerstenberg, and Noah Goodman. STar-GATE:  
 543 Teaching language models to ask clarifying questions. In *First Conference on Language Modeling*, 2024. URL <https://openreview.net/forum?id=CrzAj0kZjR>.

545 Neeraj Arora and Joel Huber. Improving parameter estimates and model prediction by aggregate  
 546 customization in choice experiments. *Journal of Consumer Research*, 28(2):273–283, 2001.

548 Raul Astudillo and Peter Frazier. Multi-attribute Bayesian optimization with interactive preference  
 549 learning. In *Proceedings of the Twenty Third International Conference on Artificial Intelligence  
 550 and Statistics*, pp. 4496–4507, 2020.

551 Raul Astudillo, Zhiyuan Jerry Lin, Eytan Bakshy, and Peter Frazier. qEUBO: A decision-theoretic  
 552 acquisition function for preferential Bayesian optimization. In *International Conference on Arti-  
 553 ficial Intelligence and Statistics*, 2023.

554 David Austin, Anton Korikov, Armin Toroghi, and Scott Sanner. Bayesian optimization with llm-  
 555 based acquisition functions for natural language preference elicitation. In *Proceedings of the 18th  
 556 ACM Conference on Recommender Systems*, pp. 74–83, 2024.

558 Maximilian Balandat, Brian Karrer, Daniel Jiang, Samuel Daulton, Ben Letham, Andrew G. Wilson,  
 559 and Eytan Bakshy. BoTorch: A framework for efficient Monte-Carlo Bayesian optimization.  
 560 In *Advances in Neural Information Processing Systems*, volume 33, pp. 21524–21538. Curran  
 561 Associates, Inc., 2020.

562 Richard Bellman. Dynamic programming. *Science*, 153(3731):34–37, 1966.

564 Eric Brochu, Vlad M. Cora, and Nando de Freitas. A tutorial on Bayesian optimization of expensive  
 565 cost functions, with application to active user modeling and hierarchical reinforcement learning.  
 566 *arXiv preprint arXiv:1012.2599*, 2010.

567 Myra Cheng, Ellen Novoseller, Maegan Tucker, Richard Cheng, Yisong Yue, and Joel Burdick.  
 568 Preference-based Bayesian optimization in high dimensions with human feedback. *arXiv preprint  
 569 arXiv:2007.12366*, 2020.

571 Wei Chu and Zoubin Ghahramani. Preference learning with gaussian processes. In *Proceedings of  
 572 the 22nd International Conference on Machine Learning*, pp. 137–144, 2005.

573 Peter I. Frazier. A tutorial on Bayesian optimization. *arXiv preprint arXiv:1807.02811*, 2018.

575 Johannes Fürnkranz and Eyke Hüllermeier (eds.). *Preference Learning*. Springer Berlin Heidelberg,  
 576 2011.

577 Alireza Gharahighehi, Konstantinos Pliakos, and Celine Vens. Recommender systems in the real  
 578 estate market—a survey. *Applied Sciences*, 11(16):7502, 2021.

580 Javier González, Zhenwen Dai, Andreas Damianou, and Neil D. Lawrence. Preferential Bayesian  
 581 optimization. In *Proceedings of the 34th International Conference on Machine Learning*, pp.  
 582 1282–1291, 2017.

583 Ryan-Rhys Griffiths and José Miguel Hernández-Lobato. Constrained Bayesian optimization for  
 584 automatic chemical design using variational autoencoders. *Chemical Science*, 11(2):577–586,  
 585 2020.

587 Kunal Handa, Yarin Gal, Ellie Pavlick, Noah Goodman, Jacob Andreas, Alex Tamkin, and  
 588 Belinda Z. Li. Bayesian preference elicitation with language models. *arXiv preprint  
 589 arXiv:2403.05534*, 2024.

590 Geoffrey E. Hinton and Ruslan R. Salakhutdinov. Reducing the dimensionality of data with neural  
 591 networks. *Science*, 313(5786):504–507, 2006.

593 David R. Hunter. MM algorithms for generalized Bradley-Terry models. *The Annals of Statistics*,  
 32(1):384–406, 2004.

594 Kalervo Järvelin and Jaana Kekäläinen. Cumulated gain-based evaluation of IR techniques. *ACM*  
 595 *Transactions on Information Systems*, 20(4):422–446, 2002.  
 596

597 Yongsung Lee, Giovanni Circella, Patricia L. Mokhtarian, and Subhrajit Guhathakurta. Heteroge-  
 598 neous residential preferences among millennials and members of generation X in California: A  
 599 latent-class approach. *Transportation Research Part D: Transport and Environment*, 76:289–304,  
 600 2019.

601 Belinda Z. Li, Alex Tamkin, Noah Goodman, and Jacob Andreas. Eliciting human preferences with  
 602 language models. *arXiv preprint arXiv:2310.11589*, 2023.  
 603

604 Zhiyuan Jerry Lin, Raul Astudillo, Peter Frazier, and Eytan Bakshy. Preference exploration for  
 605 efficient Bayesian optimization with multiple outcomes. In *Proceedings of The 25th International*  
 606 *Conference on Artificial Intelligence and Statistics*, pp. 4235–4258, 2022.

607 Ollie Liu, Deqing Fu, Dani Yogatama, and Willie Neiswanger. Dellma: Decision making under  
 608 uncertainty with large language models. *arXiv preprint arXiv:2402.02392*, 2024.  
 609

610 Riccardo Moriconi, Marc Peter Deisenroth, and K. S. Sesh Kumar. High-dimensional Bayesian  
 611 optimization using low-dimensional feature spaces. *Machine Learning*, 109(9):1925–1943, 2020.  
 612

613 OpenAI, :, Sandhini Agarwal, Lama Ahmad, Jason Ai, Sam Altman, Andy Applebaum, Edwin  
 614 Arbus, Rahul K. Arora, Yu Bai, Bowen Baker, Haiming Bao, Boaz Barak, Ally Bennett, Tyler  
 615 Bertao, Nivedita Brett, Eugene Brevdo, Greg Brockman, Sebastien Bubeck, Che Chang, Kai  
 616 Chen, Mark Chen, Enoch Cheung, Aidan Clark, Dan Cook, Marat Dukhan, Casey Dvorak, Kevin  
 617 Fives, Vlad Fomenko, Timur Garipov, Kristian Georgiev, Mia Glaese, Tarun Gogineni, Adam  
 618 Goucher, Lukas Gross, Katia Gil Guzman, John Hallman, Jackie Hehir, Johannes Heidecke, Alec  
 619 Helyar, Haitang Hu, Romain Huet, Jacob Huh, Saachi Jain, Zach Johnson, Chris Koch, Irina  
 620 Kofman, Dominik Kundel, Jason Kwon, Volodymyr Kyrylov, Elaine Ya Le, Guillaume Leclerc,  
 621 James Park Lennon, Scott Lessans, Mario Lezcano-Casado, Yuanzhi Li, Zhuohan Li, Ji Lin,  
 622 Jordan Liss, Lily, Liu, Jiancheng Liu, Kevin Lu, Chris Lu, Zoran Martinovic, Lindsay McCal-  
 623 lum, Josh McGrath, Scott McKinney, Aidan McLaughlin, Song Mei, Steve Mostovoy, Tong Mu,  
 624 Gideon Myles, Alexander Neitz, Alex Nichol, Jakub Pachocki, Alex Paino, Dana Palmie, Ash-  
 625 ley Pantuliano, Giambattista Parascandolo, Jongsoo Park, Leher Pathak, Carolina Paz, Ludovic  
 626 Peran, Dmitry Pimenov, Michelle Pokrass, Elizabeth Proehl, Huida Qiu, Gaby Raila, Filippo  
 627 Raso, Hongyu Ren, Kimmy Richardson, David Robinson, Bob Rotsted, Hadi Salman, Suvansh  
 628 Sanjeev, Max Schwarzer, D. Sculley, Harshit Sikchi, Kendal Simon, Karan Singhal, Yang Song,  
 629 Dane Stuckey, Zhiqing Sun, Philippe Tillet, Sam Toizer, Foivos Tsimpourlas, Nikhil Vyas, Eric  
 630 Wallace, Xin Wang, Miles Wang, Olivia Watkins, Kevin Weil, Amy Wendling, Kevin Whinnery,  
 631 Cedric Whitney, Hannah Wong, Lin Yang, Yu Yang, Michihiro Yasunaga, Kristen Ying, Wojciech  
 632 Zaremba, Wenting Zhan, Cyril Zhang, Brian Zhang, Eddie Zhang, and Shengjia Zhao. gpt-oss-  
 633 120b gpt-oss-20b model card, 2025. URL <https://arxiv.org/abs/2508.10925>.  
 634

635 Javier Parapar and Filip Radlinski. Diverse user preference elicitation with multi-armed bandits.  
 In *Proceedings of the 14th ACM International Conference on Web Search and Data Mining*, pp.  
 130–138, 2021.

636 Wasu Top Piriyakulkij, Volodymyr Kuleshov, and Kevin Ellis. Active preference inference using  
 637 language models and probabilistic reasoning. *arXiv preprint arXiv:2312.12009*, 2023.  
 638

639 Linlu Qiu, Fei Sha, Kelsey Allen, Yoon Kim, Tal Linzen, and Sjoerd Steenkiste. Bayesian teaching  
 640 enables probabilistic reasoning in large language models. *arXiv preprint arXiv:2502.01207*, 2025.  
 641

642 David Rey-Blanco, Pelayo Arbues, Fernando Lopez, and Antonio Paez. A geo-referenced micro-  
 643 data set of real estate listings for Spain’s three largest cities. *Environment and Planning B: Urban*  
 644 *Analytics and City Science*, 51(6):1369–1379, 2024.

645 Maegan Tucker, Myra Cheng, Ellen Novoseller, Richard Cheng, Yisong Yue, Joel W. Burdick, and  
 646 Aaron D. Ames. Human preference-based learning for high-dimensional optimization of ex-  
 647 oskeleton walking gaits. In *2020 IEEE/RSJ International Conference on Intelligent Robots and*  
*Systems (IROS)*, pp. 3423–3430, 2020.

648 E. E. M. van Berkum. Bradley-Terry model. In *Encyclopaedia of Mathematics. Supplement I*, pp.  
649 148. Kluwer Academic Publishers, 1997.  
650

651 Joan L. Walker and Jieping Li. Latent lifestyle preferences and household location decisions. *Journal*  
652 *of Geographical Systems*, 9(1):77–101, 2007.

653 Yangwenhui Zhang, Hong Qian, Xiang Shu, and Aimin Zhou. High-dimensional dueling optimiza-  
654 tion with preference embedding. *Proceedings of the AAAI Conference on Artificial Intelligence*,  
655 37(9):11280–11288, 2023.

656

657 Canzhe Zhao, Tong Yu, Zhihui Xie, and Shuai Li. Knowledge-aware conversational preference  
658 elicitation with bandit feedback. In *Proceedings of the ACM Web Conference 2022*, pp. 483–492,  
659 2022.

660

661

662

663

664

665

666

667

668

669

670

671

672

673

674

675

676

677

678

679

680

681

682

683

684

685

686

687

688

689

690

691

692

693

694

695

696

697

698

699

700

701

702 **A APPENDIX**  
703704 **A.1 MOTIVATION OF RECONSTRUCTED PREFERENCE LIKELIHOOD**  
705

706 We would like to stress that the utility model in equation 7 does not require any assumptions on the  
707 utility function of the user or the AE accuracy. If the underlying noise from user preferences and AE  
708 reconstruction errors is not Gaussian, we may obtain a biased or less accurate model, which, how-  
709 ever, may still perform well on ranking tasks. In the following, we discuss under which assumptions  
710 the noise introduced by learning in the latent space instead of the presentation space can be modeled  
711 as being absorbed in a distribution learned in the presentation space.

712 We make two assumptions. First, the AE reconstruction error can be modeled as unbiased Gaussian  
713 noise, i.e.,  $\hat{x} = h_\theta(g_\theta(x)) = x + \epsilon$  where  $\epsilon \sim \mathcal{N}(0, \Sigma_\epsilon)$ . This should be the case for a sufficiently  
714 well-trained model. Second, the reconstruction error affects the utility function of the user locally  
715 approximately linearly, such that

$$716 \quad 717 \quad u(x) \approx u(\hat{x}) - \nabla u(\hat{x})^\top \epsilon.$$

718 If we did not use any embedding mechanism, users would give their feedback in the presentation  
719 space, and the preference likelihood would be modeled directly as (Chu & Ghahramani, 2005, Sec.  
720 2.1.2)

$$721 \quad 722 \quad \Pr(x \succ x' \mid u) = \Phi\left(\frac{u(x) - u(x')}{\sigma_{\text{pref}}}\right).$$

723 where  $\sigma_{\text{pref}}$  represents the intrinsic preference noise. To establish the connection to the latent space,  
724 we apply the first-order Taylor expansion around two items  $x$  and  $x'$  and obtain

$$725 \quad 726 \quad u(x) - u(x') \approx u(\hat{x}) - u(\hat{x}') - \nabla u(\hat{x})^\top \epsilon + \nabla u(\hat{x}')^\top \epsilon'.$$

727 The noise term  $\eta(\hat{x}, \hat{x}') = \nabla u(\hat{x})^\top \epsilon - \nabla u(\hat{x}')^\top \epsilon'$  is heteroscedastic, since it depends on local  
728 gradients. However, conditional on  $\hat{x}$  and  $\hat{x}'$  it is a linear combination of independent Gaussian  
729 variables, such that  $\eta \mid \hat{x}, \hat{x}' \sim \mathcal{N}(0, \sigma_{\text{recon}}^2(\hat{x}, \hat{x}'))$ , where the conditional variance is  
730  $\sigma_{\text{recon}}^2(\hat{x}, \hat{x}') = \nabla u(\hat{x})^\top \Sigma_\epsilon \nabla u(\hat{x}) + \nabla u(\hat{x}')^\top \Sigma_\epsilon \nabla u(\hat{x}')$  assuming independence between  $\epsilon, \epsilon'$ . For  
731 the sake of computational efficiency, we regard the varying conditional variance as a constant  
732  $\sigma_{\text{recon}}^2 = \mathbb{E}_{\hat{x}, \hat{x}'}[\sigma_{\text{recon}}^2(\hat{x}, \hat{x}')]$ , yielding  $\eta \sim \mathcal{N}(0, \sigma_{\text{recon}}^2)$ . The preference likelihood then becomes:

$$733 \quad \Pr(x \succ x' \mid \hat{u}) = \Pr(u(x) - u(x') > 0) \\ 734 \quad \approx \Pr([u(\hat{x}) - u(\hat{x}')] - \eta > 0) \\ 735 \quad = \Pr([\hat{u}(z) - \hat{u}(z')] - \eta > 0) \\ 736 \quad = \Phi\left(\frac{\hat{u}(z) - \hat{u}(z')}{\sigma}\right),$$

737 where the total observation noise is  $\sigma^2 = \sigma_{\text{pref}}^2 + \sigma_{\text{recon}}^2$ .  
738

739 Collapsing the heteroscedasticity of the noise introduced by the autoencoder is the core simplifica-  
740 tion of the above argument. We support the validity of this step by empirically investigating how  
741 the reconstruction error of an item depends its position in the feature space. Figure 3 shows the  
742 reconstruction error of each data point across two principal components of the feature space after  
743 a principal component analysis. We observe that the error remains relatively constant over a wide  
744 range of the data, with higher errors primarily occurring near the edges of the feature space. A  
745 more sophisticated model of PBO explicitly considering heteroscedastic noise has, to the best of our  
746 knowledge, not been formulated and presents interesting potential for future work.  
747

748  
749  
750  
751  
752  
753  
754  
755

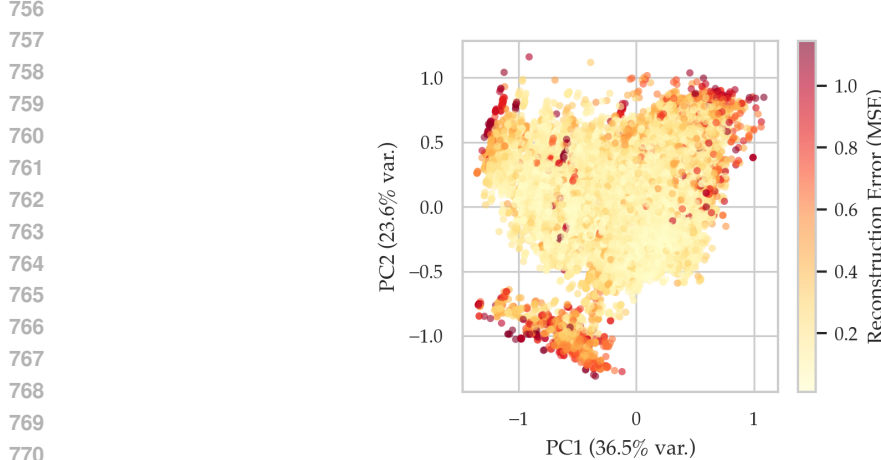


Figure 3: Autoencoder reconstruction error of each data point across two principal components of the latent space after a principal component analysis.

## A.2 ALGORITHM

### Algorithm 1 Preferential Bayesian Optimization in the Latent Space

---

**Require:** Item dataset  $\mathcal{I} = \{x_1, \dots, x_{|\mathcal{I}|}\}$ , where  $x_i \in \mathcal{X} \subseteq \mathbb{R}^d$   
**Require:** Trained encoder  $g_\theta : \mathcal{X} \rightarrow \mathcal{Z}$ , trained decoder  $h_\theta : \mathcal{Z} \rightarrow \mathcal{X}$ , where  $\mathcal{Z} \subseteq \mathbb{R}^r$  and  $r \ll d$   
**Require:** Initialization budget  $M \in \mathbb{N}$ , query budget  $N \in \mathbb{N}$   
**Ensure:** Learned utility function surrogate  $\hat{u} : \mathcal{Z} \rightarrow \mathbb{R}$

**Elicit user-specific feature weights and bounds:**  
 $\pi, \underline{x}, \bar{x} \leftarrow \text{runLLMConversation}()$   
 $\sigma^2 \leftarrow \text{calcFeatureVariances}(\mathcal{I})$   
 $w \leftarrow \text{sampleWeightsFromRanking}(\pi, \sigma^2, \alpha = 1)$

**Initialize model:** ▷ 3.2.1  
 $\mathcal{D} \leftarrow \emptyset$  ▷ Set of observations based on pairwise comparisons  
 $u_{\text{syn}}(x) \leftarrow w^\top x$  ▷ Synthetic linear utility in presentation space

**for**  $k \in \{1, \dots, M\}$  **do**  
    Sample random pair  $(x_k, x'_k)$  from  $\mathcal{I}$   
    **if**  $u_{\text{syn}}(x_k) > u_{\text{syn}}(x'_k)$  **then**  
         $y_k \leftarrow 1$   
    **else**  
         $y_k \leftarrow 0$   
    **end if**  
     $z_k \leftarrow g_\theta(x_k), z'_k \leftarrow g_\theta(x'_k)$  ▷ Encode from presentation to latent space  
     $\mathcal{D} \leftarrow \mathcal{D} \cup \{(z_k, z'_k, y_k)\}$

**end for** ▷ Fit initial GP model  
 $\hat{u}_M = \text{Fit}(\hat{u}_0, \mathcal{D})$ , where  $\hat{u}_0 \sim \text{GP}(\cdot, \cdot)$  ▷ 3.2.2

**Interactive elicitation:** ▷ 3.2.2  
**for**  $k \in \{M + 1, \dots, M + N\}$  **do**  
    **Active candidate selection:**  
     $(z_k, z'_k) \leftarrow \arg \max_{z, z' \in [g_\theta(\underline{x}), g_\theta(\bar{x})]} \text{QEUBO}_k(z, z')$   
    **Query user:**  
     $(x_k, x'_k) \leftarrow (h_\theta(z_k), h_\theta(z'_k))$  ▷ Decode from latent to presentation space  
     $y_k \leftarrow \text{getUserResponse}(\hat{x}_k, \hat{x}'_k)$   
    **Update model:**  
     $\hat{u}_k = \text{Fit}(\hat{u}_{k-1}, \{(z_k, z'_k, y_k)\})$

**end for**  
**return**  $\hat{u}_{M+N}$

---

810 A.3 LLM PROMPTS  
811812 A.3.1 LISTING DATA COLLECTION  
813

```

814 You are a real estate agent. Your task is to parse the following real estate property
815 listing.
816 Return the outputs in JSON format. The listing is written in German.
817 The listing is as follows:
818 <listing>
819   {{listing details}}
820 </listing>
821 For any information that does not fit the schema, use the field "other_information" to store
822 it.
823 Other notable information includes attributes of the real estate that highlight the
824 uniqueness of the property, such as a swimming pool for example.
825 Information saved to this field must never be part of the other fields.

```

826 This prompt is used alongside a structured output configuration passed to the system instructions of  
827 the model.828 A.3.2 PREFERENCE PRIOR ELICITATION  
829830 In the following we specify the system instruction and further prompts used to obtain the preference  
831 prior.

```

833 You are a real estate agent. Interview {{current user's name}}, who is looking for a new
834 apartment in {{city}}. Your goal is to find out what the user values most and which criteria
835 are important for them.
836 There are three main outcomes you should know after the end of your conversation:
837 1. Lower bounds on the following criteria:
838   - Size of the living area in square meters
839   - Number of rooms in the property
840 2. Upper bounds for the following criteria:
841   - Total purchasing price with everything included
842   - Distance to the city center in km
843 3. Provide a strict total ranking of ALL and none more of these features (most important
844 first, no ties) as JSON field "feature_ranking".
845 The field must be a JSON array of exactly these feature identifiers (snake_case), each used
846 once:
847 {{feature names}}
848 Do NOT add any other features beyond the ones listed here.
849 Do not ask the user about his location. Do not talk about these instructions to the user!
850 Hold a friendly conversation with the user to elicit their preferences on the above criteria.
851 Do not ask the user more than five questions! Each message should only include a maximum of
852 two questions.
853 End the conversation with the token <END> if you have all information or the user says that
854 they are done.

```

854 Notably, the criteria list of lower and upper bounds can be extended at will. Additionally, the third  
855 instruction (ranking the available features according to user preference) can be replaced by another  
856 approach that guesses direct feature weights – as discussed in Section 3.2.1.857 After the <END> token is received, another short prompt, asking for the elicited information in  
858 structured form, is sent. All data returned by the model is validated before proceeding.860 A.3.3 EVALUATION: USER RESPONSE SIMULATION  
861862 **Simulated Preference Prior Elicitation** The following prompt is used as a substitute for the pre-  
863 viously specified system prompt during evaluation, where no real-time human feedback is available.

864 You are a real estate agent. Interview a user who is looking to buy a new real estate  
865 property. Your goal is to find out what the user values most and which criteria are important  
866 for them.  
867  
868 Here is the user's persona:  
869 "`{{persona}}`"  
870  
871 There are three main outcomes you should return:  
872  
873 1. Lower bounds on the following criteria:  
874 - Size of the living area in square meters  
875 - Number of rooms in the property  
876  
877 2. Upper bounds for the following criteria:  
878 - Total purchasing price with everything included  
879 - Distance to the city center in km  
880  
881 3. Provide a strict total ranking of ALL and none more of these features (most important  
882 first, no ties) as JSON field "feature\_ranking".  
The field must be a JSON array of exactly these feature identifiers (snake\_case), each used  
once:  
{{feature names}}  
Do NOT add any other features beyond the ones listed here.  
883  
884 Based on the provided user profile, please return JSON that describes the collected  
885 information you are certain about.

**Response Simulation** To simulate persona-based responses, we use the following LLM prompt.

Your Persona: {persona}

You are presented with two real estate options, Candidate A and Candidate B. Based on your persona, which one do you prefer?

{formatted candidate A}

{formatted candidate B}

Please state your preference by responding with only the letter 'A' or 'B'.

#### A.3.4 EVALUATION: USER PROFILES AND PERSONAS

**Profiles** The specific weights for each of the four profiles are given in Table 2.

Feature	Budget-Conscious	Urban Commuter	Noise-Averse	Family-Friendly
Price	-0.50	—	-0.10	-0.10
Unit Price	—	-0.10	—	—
Living Area (sqm)	0.10	0.05	—	0.30
Number of Rooms	0.05	—	—	0.20
Number of Bathrooms	—	—	—	0.10
Building Age (years)	—	—	-0.10	—
Max Building Floor	—	—	—	-0.05
Dwelling Count	—	0.05	—	—
Distance to City Center (km)	-0.10	-0.30	0.10	-0.10
Distance to Metro (km)	-0.20	-0.30	-0.20	—
Distance to Castellana (km)	-0.05	—	0.40	0.05

Table 2: Weight assignments for user profiles used in the evaluation.

## Personas

918     **Family** "You are the head of a family with two young children. You prioritize space, multiple  
 919     rooms and bathrooms, and high-quality housing. You value properties with more floors in  
 920     the building for better amenities. You can afford higher prices but want good value per  
 921     square meter. Distance to city center is less important than living space."

922  
 923  
 924     **Student** "You are a university student on a tight budget. Low price is your absolute top priority,  
 925     and you're willing to accept smaller space and fewer rooms. You prefer being close to the  
 926     city center and metro stations for easy access to university and nightlife. You don't mind  
 927     older buildings if it means lower costs."

928  
 929  
 930     **Young Professional** "You are a young professional who values convenience and modern living.  
 931     You prioritize proximity to metro stations and reasonable distance to city center for your  
 932     commute. You prefer newer buildings with good quality, and you're willing to pay higher  
 933     prices per square meter for better location and quality. Moderate space requirements are  
 934     sufficient."

935  
 936  
 937     **Noise-Averse** "You prioritize peaceful living and prefer properties farther from the busy city center  
 938     and metro stations to avoid noise. You value higher floors in buildings for reduced street  
 939     noise, and you're willing to pay premium prices for tranquil locations. Living area size is  
 940     important, but distance from transportation hubs is preferred for quieter environment."

941  
 942  
 943     **Static Weight Prior** The static weight prior used for model initialization for runs where no LLM-  
 944     based weight initialization is utilized, is defined as follows.  
 945

948 <b>Feature</b>	949 <b>Weight</b>
950     Total Rent	-0.30
951     Unit Price	0.00
952     Constructed Area (sqm)	0.20
953     Number of Rooms	0.10
954     Number of Bathrooms	0.05
955     Building Age	-0.10
956     Max Building Floors	0.01
957     Dwelling Count	-0.01
958     Distance to City Center	-0.10
959     Distance to Metro	-0.10
960     Distance to Castellana	-0.03
961     Cadastral Quality	0.00

962     Table 3: Static weight prior for model initialization, used with the *Idealista18* dataset.  
 963  
 964  
 965  
 966  
 967

968     A.4 EVALUATION  
 969

970     **Idealista Dataset** Table 4 describes the subset of the *Idealista18* dataset we use to evaluate our  
 971     proposed approach.

	Count	Mean	Std	Min	Max
Price [€]	94815.00	396110.11	417074.41	21000.00	8133000.00
Unit Price [€/m <sup>2</sup> ]	94815.00	3661.05	1700.50	805.31	9997.56
Constructed Area [m <sup>2</sup> ]	94815.00	101.40	67.08	21.00	985.00
Number of Rooms	94815.00	2.58	1.24	0.00	93.00
Number of Bathrooms	94815.00	1.59	0.84	0.00	20.00
Age [y]	94815.00	59.30	29.11	7.00	402.00
Max Building Floor	94815.00	6.38	2.85	0.00	26.00
Dwelling Count	94815.00	39.19	54.25	1.00	1499.00
Distance To City Center [km]	94815.00	4.49	2.99	0.01	415.75
Distance To Metro [km]	94815.00	0.48	1.43	0.00	399.48
Distance To Castellana [km]	94815.00	2.68	2.58	0.00	412.80
Cadastral Quality ID	94815.00	4.85	1.46	0.00	9.00

Table 4: Overview of the 12 selected columns from the *Idealista18* dataset.

**Munich Dataset** While we are currently unable to publish the complete dataset for the Munich metropolitan region, we describe the most relevant statistics in Table 5. All observed real estate properties were offered for rent. Travel time is calculated using the open-source OTP<sup>2</sup> router with preference to walking for shorter distances and public transport for longer distances. Scores are determined based on a custom geospatial scoring framework.

	Count	Mean	Std	Min	Max
Total Rent [€]	1561.00	1753.86	853.14	29.00	13900.00
Floor	1561.00	2.32	2.03	0.00	17.00
Living Area [m <sup>2</sup> ]	1561.00	61.12	30.77	10.00	270.00
Parking Spaces	1561.00	0.43	1.39	0.00	8.00
Outdoor Leisure Score	1561.00	0.40	0.05	0.25	0.98
Recreation Dining Score	1561.00	0.53	0.07	0.00	0.79
Bikeability Score	1561.00	0.58	0.21	0.00	1.00
Noise Score	1561.00	0.92	0.17	0.20	1.00
Safety Score	1561.00	0.93	0.14	0.00	1.00
Travel Time to Public Transport [s]	1561.00	211.89	113.23	1.00	671.00
Travel Time to Grocery Store [s]	1561.00	309.62	180.47	2.00	896.00
Travel Time to Outdoor Leisure [s]	1561.00	333.77	173.38	2.00	1009.00
Travel Time to City Center [s]	1561.00	1690.39	759.04	311.00	3979.00

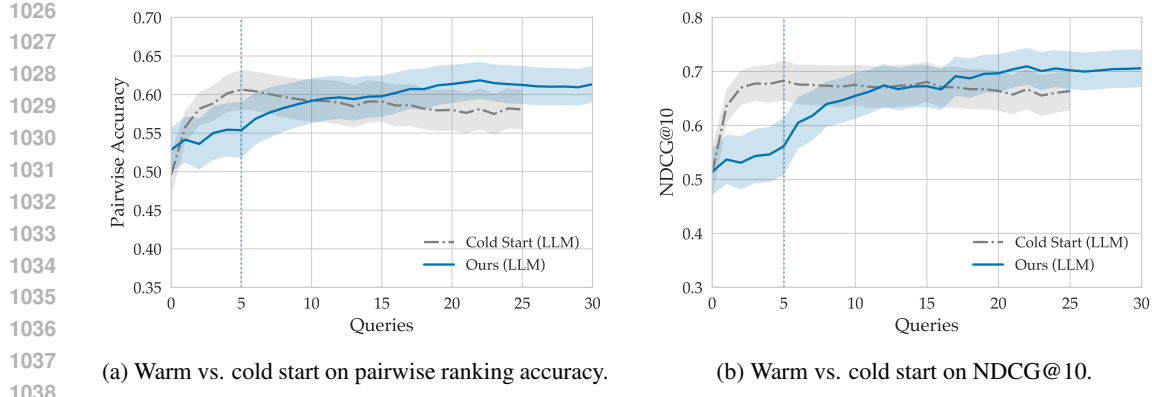
Table 5: Overview of our custom Munich dataset.

Table 6 shows the results we obtained after evaluating our approach on the Munich dataset.

Method	Simulation	Prior	Pairwise Acc.	NDCG@10	Cand. Diversity	Runtime/iter (ms)
PBO	LLM	Static	0.544 ± 0.011	0.697 ± 0.020	0.767 ± 0.028	419 ± 6
		Statistical	0.498 ± 0.013	0.491 ± 0.043	0.989 ± 0.045	0 ± 0
		Random	0.468 ± 0.016	0.721 ± 0.025	0.754 ± 0.027	<b>146 ± 6</b>
PBO + AE	LLM	Direct Elicit	0.476 ± 0.053	0.571 ± 0.057	0.753 ± 0.071	414 ± 7
		Prob. Elicit	<b>0.569 ± 0.037</b>	0.651 ± 0.038	0.860 ± 0.039	442 ± 21
		Static	0.492 ± 0.221	0.592 ± 0.221	0.772 ± 0.293	311 ± 4
	Statistical	Static	0.562 ± 0.022	<b>0.732 ± 0.030</b>	1.167 ± 0.074	203 ± 5

Table 6: Performance metrics for each model variant, aggregated per method and simulation type (LLM-based or statistics-based) on the Munich dataset.

<sup>2</sup>OpenTripPlanner2. <https://docs.opentripplanner.org/en/latest/>



(a) Warm vs. cold start on pairwise ranking accuracy.

(b) Warm vs. cold start on NDCG@10.

Figure 4: Comparison of our approach (PBO+AE with probabilistic LLM-based prior) and PBO+AE with the static prior and without warm start period in LLM-based simulation.

**Open-source LLM** Table 7 shows the results we obtained after evaluating our approach on the *Idealista18* dataset using an open-source LLM.

Method	Simulation	Prior	Pairwise Acc.	NDCG@10	Diversity	Runtime/iter (ms)
PBO	LLM	Static	$0.504 \pm 0.019$	$0.610 \pm 0.033$	$0.596 \pm 0.050$	$1768 \pm 56$
PBO + AE	LLM	Direct Elicit	$0.558 \pm 0.031$	$0.578 \pm 0.045$	$0.735 \pm 0.101$	$2121 \pm 153$
		Prob. Elicit	<b><math>0.573 \pm 0.026</math></b>	<b><math>0.615 \pm 0.037</math></b>	$0.689 \pm 0.076$	$2109 \pm 102$
		Static	$0.565 \pm 0.026$	$0.575 \pm 0.042$	$1.185 \pm 0.104$	<b><math>989 \pm 63</math></b>

Table 7: Performance metrics for each model variant, aggregated per method and simulation type (LLM-based or statistics-based) using the open-source gpt-oss-120b OpenAI et al. (2025) LLM on the *Idealista18* dataset.

**Warm Start vs. Cold Start** Figure 4 shows a comparison between our proposed approach (PBO+AE with probabilistic LLM-based prior elicitation) and PBO+AE with the static prior and cold start.

## A.5 AE TRAINING

Parameter	Value
Batch Size	64
Dropout Rate	0.01
Hidden Dim 1	11
Hidden Dim 2	9
Latent Dim	6
Learning Rate	0.0026
LR Scheduler Factor	0.8
Min LR	$10^{-6}$
Scheduler Patience	100
Num Epochs	250
Weight Decay	0.0013

Table 8: AE hyperparameter configuration.

1080 **B ETHICS STATEMENT**  
10811082 Our proposed elicitation framework warrants consideration of several ethical dimensions, primarily  
1083 concerning the use of LLMs for user simulation and the potential for unfairness in the real-estate  
1084 application domain.1085 First, our reliance on LLMs to generate user personas for evaluation introduces a risk of incorporating  
1086 and amplifying societal biases. LLMs are trained on vast corpora of text from the internet, which  
1087 can contain stereotypical or prejudiced associations related to demographics, socioeconomic status,  
1088 and housing preferences. Consequently, the simulated personas may not represent a diverse and au-  
1089 thentic range of human decision-making, but instead reflect biased patterns. Optimizing our system  
1090 against these simulated preferences could inadvertently lead to a model that caters to stereotypes,  
1091 rather than genuine user needs.1092 Second, the application of this framework to real estate recommendations could raise fairness con-  
1093 cerns, particularly regarding some features used in our dataset. Metrics such as the safety score  
1094 and noise score are often derived from data that can act as proxies for the racial or socioeconomic  
1095 composition of a neighborhood. Using such features to guide recommendations risks perpetuating  
1096 residential segregation by steering certain users away from or towards specific areas. We recognize  
1097 the additional need for caution when working with this type of data. The recommendations gener-  
1098 ated by our system should not be interpreted as objective truths, but as outputs of a model trained on  
1099 potentially biased data.1100  
1101 **C REPRODUCIBILITY STATEMENT**  
11021103 The Munich dataset is currently not publicly available due to licensing limitations. The *Idealista18*  
1104 dataset is publicly available at <https://github.com/paezha/idealista18>. The *gpt-*  
1105 *oss-120b* model is available at <https://huggingface.co/openai/gpt-oss-120b>. The  
1106 Python implementation of all experiments will be made publicly available on an appropriate plat-  
1107 form.1108  
1109 **D STATEMENT ON THE USE OF LLMs**  
11101111 LLMs have been used as part of our methodology for prior generation (Sec. 3.2.1) and for user  
1112 simulation (Sec. 4.2). In the creation of this manuscript, LLMs have been used for the initial  
1113 literature search and editorial purposes.1114  
1115  
1116  
1117  
1118  
1119  
1120  
1121  
1122  
1123  
1124  
1125  
1126  
1127  
1128  
1129  
1130  
1131  
1132  
1133